ICSO 2016

International Conference on Space Optics

Biarritz, France

18–21 October 2016

Edited by Bruno Cugny, Nikos Karafolas and Zoran Sodnik

Mechanical stress in dielectric mirrors: towards a fine control of the flatness

Thomas Begou

Julien Lumeau

icso proceedings

International Conference on Space Optics — ICSO 2016, edited by Bruno Cugny, Nikos Karafolas,
Zoran Sodnik, Proc. of SPIE Vol. 10562, 105621F · © 2016 ESA and CNES
CCC code: 0277-786X/17/$18 · doi: 10.1117/12.2296090

Mechanical stress in dielectric mirrors: towards a fine control of the flatness

Thomas Begou and Julien Lumeau
Aix-Marseille Université, CNRS, Centrale Marseille, Institut Fresnel, UMR 7249, 13013 Marseille - France
thomas.begou@fresnel.fr

INTRODUCTION

Today, the demand on flat optical components with specification on final surface flatness that must be smaller than $\lambda/20$ or $\lambda/30$ peak to valley, for various applications including linear accelerators [1,2], space applications [3]…, needs an accurate knowledge on the mechanical stress induced in thin films. In order to design correctly stacks of thin films on both side of a substrate and achieve perfect stress compensation, it is thus obvious that the first step is to precisely characterize the stress in single layers. Then from the characterization of single layer, we can model stress induced in multlilayers and develop strategies to optimize the stack design on both sides of the substrate to control the flatness of the final component.

I. EXPERIMENTAL SET UP

All the optical components were manufactured with the help of a HELIOS 4" machine, developed by Bühler/Leybold Optics, where low and high refractive index materials were both deposited through Plasma Assisted Reactive Magnetron Sputtering (PARMS) [4,5]. As seen in Fig. 1., the main chamber of the machine is subdivided in 4 deposition/treatment zones, two dedicated for dielectric materials (mid frequency (MF) magnetron sputtering), one for metallic deposition (DC magnetron sputtering, not used here) and the last one for oxygen plasma assistance (PBS).

The substrates are set on a 12-position rotating sample holder (rotating at 240 rpm). According to the deposited material, either low or high refractive index, the corresponding MF magnetron sputtering cathode is switched on; the oxygen plasma assistance is used for densification of the coating and also to respect the stoichiometry of the layers. Typical deposition rates of low and high index materials are respectively around 0.40-0.45 nm.s^{-1} and 0.50-0.60 nm.s^{-1}, which means that less than an atomic layer of material is deposited at each turn of the sample holder. Thicknesses of the different deposited layers are optically controlled, in a transmission mode, at a precisely selected wavelength through the Optical Monitoring System OMS5000 developed by Bühler/Leybold Optics [6].

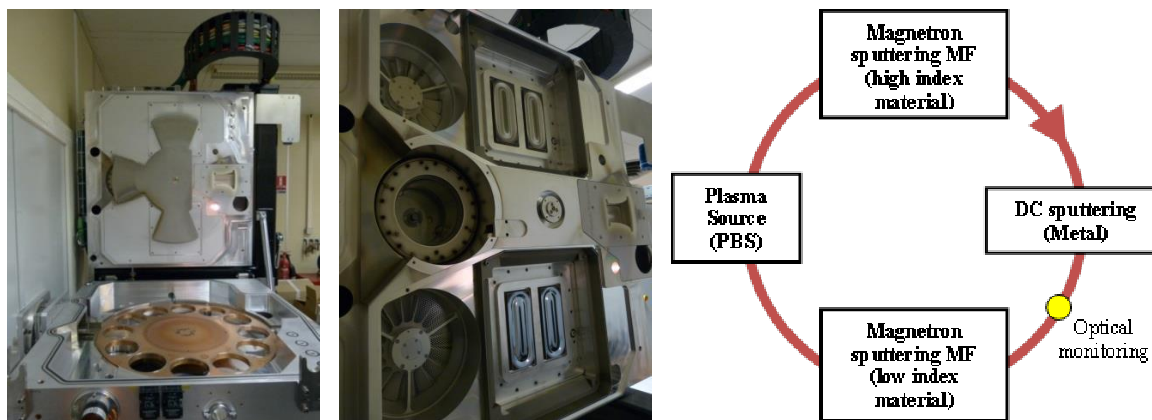

Fig. 1. HELIOS deposition process chamber.

Mechanical stress was then extracted from the substrate radius of curvature evolution before and after films deposition. These radiuses of curvature were measured with white light interferometry (Zygo NewView 7300).

II. STRESS IN SINGLE LAYERS

Single layers made of SiO_2 and Nb_2O_5 with different thicknesses have been deposited. For each deposition, substrate thicknesses $\boldsymbol{t_S}$ were measured with a digital micrometer and radii of curvature on both sides of the substrate, before ($\boldsymbol{R_S}$) and after ($\boldsymbol{R_{S+f}}$) deposition, were measured with white light interferometry. Stoney equation [7] (equation 1) was redefined to simply extract the information on the stress value (equation 2). In this

study, the substrates were made of fused silica (***Φ*** = 25 mm), where the Young modulus $\boldsymbol{E_s}$ = 73 GPa, the Poisson coefficient $\boldsymbol{v_s}$ = 0.16 and the thickness $\boldsymbol{t_s}$ = 1.00±0.05 mm.

$$\sigma = \frac{E_S t_S^2}{6t_f(1-\upsilon_S)}\left(\frac{1}{R_{S+f}} - \frac{1}{R_S}\right) \quad (1)$$

$$\frac{K_S}{R_{Norm}} = \sigma(t_f)t_f \quad (2)$$

In equation (2), - $\mathrm{K_S} = \frac{\mathrm{E_S}}{6(1-\upsilon_S)}$ is a constant term that depends on the mechanical properties of the substrate,

- $\mathrm{R_{Norm}} = \frac{\mathrm{R_S\,R_{S+f}}}{\mathrm{t_S}^2(\mathrm{R_S}-\mathrm{R_{S+f}})}$ is the substrate thickness normalized radius of curvature directly induced by the deposited layer.

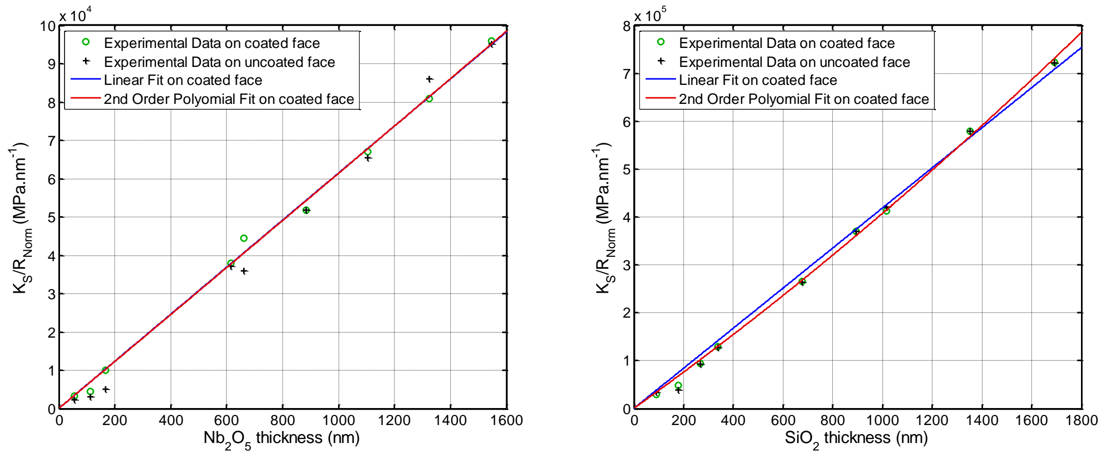

Fig. 2. Normalized radius of curvature evolution as a function of the film thickness for Nb_2O_5 (left) and SiO_2 (right). Linear fit (blue line) and second order polynomial fit (red line).

As we plotted, in Fig.2, the term $\boldsymbol{K_S/R_{Norm}}$ as a function of film thickness for both SiO_2 and Nb_2O_5 layers, we could perform two different fits on the experimental data. In a first time, we could consider a linear evolution of the data that means a constant value of the mechanical stress as a function of the film thickness: $\boldsymbol{\sigma_i} = \boldsymbol{K_i}$ [8] (***i*** stands for either SiO_2 or Nb_2O_5). In a second time we used a second order polynomial to fit the experimental data, we obtained a slightly better fit with a thickness dependence (expressed in nanometers) of the stress: $\boldsymbol{\sigma_i} = \boldsymbol{A_i} + \boldsymbol{B_i}\,\boldsymbol{t_i}$. The results of both fits are detailed in Tab. 1.

The merit function to determine the quality of the fit is described hereafter in equation 3, in which ***N*** is the number of points and ***X*** stands here for $\boldsymbol{K_S/R_{Norm}}$:

$$MF = \frac{1}{N}\sqrt{\sum_{i=1}^{N}\frac{4\left(X_{mod}-X_{exp}\right)^2}{\left(X_{mod}+X_{exp}\right)^2}} \quad (3)$$

Tab. 1. Stress parameters obtain from a linear fit and from a second order polynomial fit.

Material	Linear fit		2nd order polynomial fit		
	K	*MF*	*A*	*B*	*MF*
Nb_2O_5	**61.4**	0.051	**61.0**	**0.0003**	0.050
SiO_2	**418.5**	0.061	**371.2**	**0.0360**	0.042

III. STRESS IN MULTILAYERS

Based on the results obtained on single layers of high and low refractive index materials, we analyzed if those one can be applied to multilayer structures. We studied the evolution of stress while fabricating a mirror centered at 515 nm with R>99.95% for both ***s*** and ***p*** polarization with an angle of incidence of 22°. The designed mirror is a 21-layer quarter-wave mirror centered at 532 nm (**(HL)^{10} H**), with Nb_2O_5 as high index material and SiO^2 as low index material.

In order to test the different models of the stress in single layers, we inserted several substrates in the deposition machine and removed progressively samples to obtain mirrors with an increasing number of layers (M5, M9,

M11, M15, M17, M19 and M21) and therefore characterized the mirror deformation during its construction. This approach is possible with the HELIOS machine thanks to the load-lock that allows removing some of the samples being coated, without opening the whole deposition chamber and therefore without affecting the other samples being coated. With this procedure, all the samples were processed within the same batch.

In order to model the experimental data, we assumed that the $\boldsymbol{K_S/R_{Norm}}$ ratio evolves as expressed in equation 4 ***NH*** and ***NL*** are respectively the number of high (***H***) and low (***L***) refractive index material layers in the structure.

$$\frac{K_S}{R_{Norm}} = \sum_{i=1}^{NH} \sigma_H(t_{Hi}) t_{Hi} + \sum_{j=1}^{NL} \sigma_L(t_{Lj}) t_{Lj} \tag{4}$$

In order to have a better idea of this ratio, we focused our study on the sag of the sample after deposition. In that case, we could write again equation 4 in a different way to extract the experimental value of $\boldsymbol{R_{Norm}}$ (equation 5).

$$R_{Norm} = \frac{K_S}{\sum_{i=1}^{NH} \sigma_H t_{Hi} + \sum_{j=1}^{NL} \sigma_L t_{Lj}} \tag{5}$$

Then from this experimental normalized radius of curvature we could calculate the sag as shown in equation 6 with the sign norm described in figure 3.

$$\delta = R_{Norm} \pm \sqrt{{R_{Norm}}^2 - \left(\frac{D_S}{2}\right)^2} \tag{6}$$

In equation 5, + sign will be used if $\boldsymbol{R_{Norm}}$ is positive and – sign if $\boldsymbol{R_{Norm}}$ is negative.

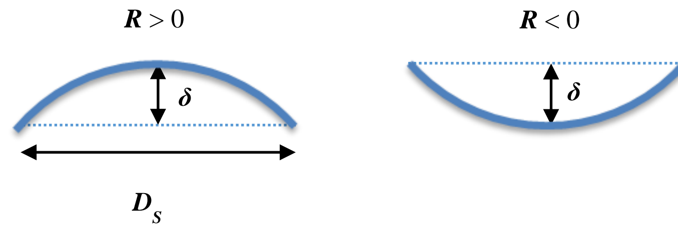

Fig.3. Definition of the sample sag $\boldsymbol{\delta}$ induced by the stress due to the deposited layers.

In Fig. 4, we plotted the experimental data measured at different steps of the mirror under fabrication on both sides of the substrate and we compared them with both models described in section 2 of this paper. The model with a thickness dependency of the stress is validated (***MF*** = 0.017) as it allows accurately predicting the stress-induced sag, while the model with constant stress values overestimates the deformation as it supposes a larger value of the stress induced that would be expected in thicker layers (***MF*** = 0.024). From this accurate model, it is now possible to precisely model the stress induced deformation by any single or multilayer structures.

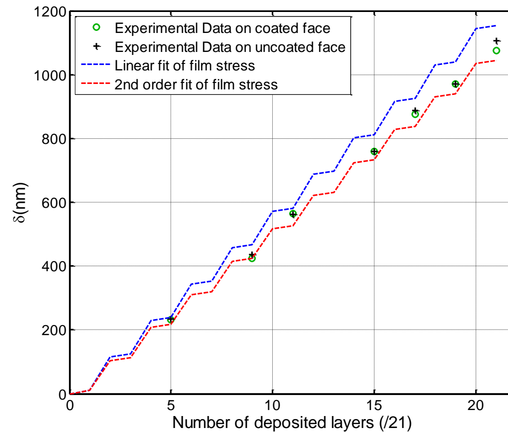

Fig.4. Evolution of $\boldsymbol{K_S/R_{Norm}}$ as a function of the number of deposited layers for a M21 mirror centered at 532 nm. Comparison between experimental data and models.

IV STRESS COMPENSATION

For many advanced applications requiring complex optical filters, one of the requirements is the flatness of the component after fabrication. In order to obtain stress compensation in multilayer optical elements, one of the

common approaches consists of depositing two optical functions with similar stress-induced deformation, on each faces of the substrate [9]. To achieve, the stress compensation should respect the equation 7.

$$\left[\sum_{i=1}^{NH}\sigma_H(t_{Hi})t_{Hi}+\sum_{j=1}^{NL}\sigma_L(t_{Lj})t_{Lj}\right]Face\ A=\left[\sum_{i=1}^{NH}\sigma_H(t_{Hi})t_{Hi}+\sum_{j=1}^{NL}\sigma_L(t_{Lj})t_{Lj}\right]Face\ B \quad (7)$$

Supposing an already A coated face, to fulfill the requirements of equation 7, there are a wide range of possible solutions for the B-face coating.

- **compensation** with a single layer of SiO_2 or Nb_2O_5 with adapted thickness,
- **compensation** with the same deposition on both sides of the substrate,
- **compensation** with an adapted AR coating [9],
- **…**

We considered in this paper, the first two different approaches:

A. Stress compensation with a single layer

Let us suppose that the face A has already been coated with the previously defined mirror (M21 @ 532 nm), equation 7 can be matched with the deposition of one single layer of SiO_2 or Nb_2O_5 that compensates the face A. In that case, equation 7 can be written as equation 8 in which $\boldsymbol{x}$ can stand either for SiO_2 or Nb_2O_5.

$$\left[\sum_{i=1}^{NH}\sigma_H(t_{Hi})t_{Hi}+\sum_{j=1}^{NL}\sigma_L(t_{Lj})t_{Lj}\right]Face\ A=\left[\sigma_X(t_X)t_X\right]Face\ B \quad (8)$$

If we assume a second order polynomial model for the stress induced by the layers, we have to solve equation 9.1 (if we consider theoretical data) or 9.2 (if we consider experimental stress measurements on the sample after deposition on face A) to find the thickness t_x of material that will compensate the deformation on the opposite face.

$$\left[\sum_{i=1}^{NH}\sigma_H(t_{Hi})t_{Hi}+\sum_{j=1}^{NL}\sigma_L(t_{Lj})t_{Lj}\right]Face\ A=\left[A_x t_x+B_x {t_x}^2\right]Face\ B \quad (9.1)$$

$$\left[\frac{K_S}{R_{Norm}}\right]Face\ A=\left[A_x t_x+B_x {t_x}^2\right]Face\ B \quad (9.2)$$

As an example, we used this method to compensate the native deformation of a bare substrate with typical deformations in the range of $\lambda/4$ peak to valley at 532 nm. In Fig.5, we show the result of the minimization of the substrate deformation on face A with an optimized thickness of SiO_2 ($\boldsymbol{t_{SiO2}}$ = 42 nm) deposited on face B. The optimized thickness of SiO_2 was calculated from equation 9.2 considering one layer of SiO_2 and an infinite value of $\boldsymbol{R_{S+f}}$ since it is a bare substrate. The radius of curvature before deposition were respectively of -986 m and -732 m for face A and B and after deposition we measured a radius of curvature of -34000 m for face A and -419 m for face B. If we calculate the residual radius of curvature on face B according to the initial radius of curvature and the thickness of the SiO_2 layer deposited on face A, we obtained -419.9 m which is in a very good agreement with experimental data.

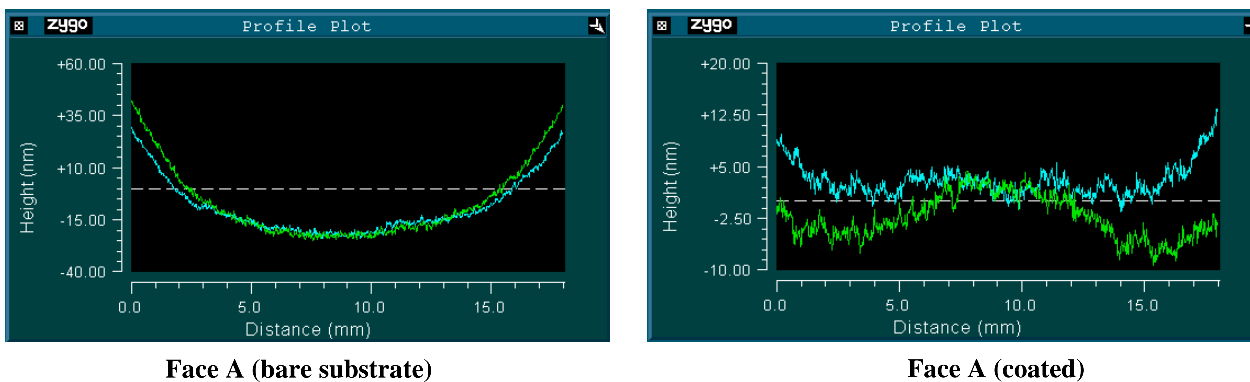

Face A (bare substrate) **Face A (coated)**

Fig.5. Deformation, on orthogonal direction, of a substrate before and after deposition of a SiO_2 compensating layer.

However, this solution works for a restricted range of temperature and does not allow controlling the spectral properties of the face B. Another solution is to deposit the same mirror on the second face.

B. Stress compensation with a multilayer

When it's possible, depending on the spectral properties of the final component, the simplest way to obtain a good compensation of the stress in the sample is to deposit the same structure on both face of the substrate. This is for example the case for highly reflecting mirrors which back face has minimal contribution to the overall spectral response of the component except if Fabry-Perot filter is created (got our application, incoherent light is used and this effect is prevented). In that case, equation 7 is respected and stress compensation is matched on a wide range of temperature (up until physical properties are changed). In that case, initial flatness of the substrate is obtained in first approximation after complete fabrication of the element. It is important to note that due to boundary conditions, a small deformation can be observed in final experimental components.

We tested this approach on two different mirrors, both were made with 21 quarter wavelength layers alternating high and low refractive index material but one is centered at 532 nm (as the one in part 3) and the other at 1053 nm. Experimental and modeled sag values of the samples are summed up in Tab .2.

First of all, as one can see in Tab. 2, the values of the sample sag after deposition on both sides are quite close to the ones of the bare substrates. The difference between the values can be explained by experimental uncertainties resulting from the measurement of small sag values, or high values of radius of curvature.

Tab. 2. Sag measured on experimental samples and simulated using both models (Linear fit and polynomial fit) for a two different mirrors (M21 @ 532 nm and M21 @ 1053 nm).

M21@532 nm **M21@1053 nm**	$\delta_{Bare\ Substrate}$ (nm)		$\delta_{1\ Face\ coated}$ (nm)		$\delta_{2\ Face\ coated}$ (nm)	
	Face A	Face B	Face A	Face B	Face A	Face B
Experimental Data	**-113.1** **-57.4**	**-104.9** **3.2**	**859.9** **1973.7**	**-1163.7** **-2031.1**	**-84.9** **-51.1**	**-131.4** **-3.7**
Linear Fit Model	**0** **0**	**0** **0**	**1154.1** **2318.7**	**-1154.1** **-2318.7**	**0** **0**	**0** **0**
Polynomial Fit Model	**0** **0**	**0** **0**	**1043.7** **2114.0**	**-1043.7** **-2114.0**	**0** **0**	**0** **0**

To compare both models with experimental data, we took into account the initial sag of the bare substrates, i.e. we subtracted the value of the initial sag to the values of the sag after coating of the face A (Tab. 3).

Tab. 3. Sag measured on experimental samples, taking account of initial deformation of the substrate, and simulated using both models (Linear fit and polynomial fit) for a two different mirrors (M21 @ 532 nm and M21 @ 1053 nm).

M21@532 nm **M21@1053 nm**	$\delta_{1\ Face\ coated}$ (nm)		**Errors between models and experimental results**	
	Face A	Face B	Face A	Face B
Experimental Data	**973.0** **2031.1**	**-1058.8** **-2034.3**		
Linear Fit Model	**1154.1** **2318.7**	**-1154.1** **-2318.7**	**-17%** **-13%**	**-9%** **-13%**
Polynomial Fit Model	**1043.7** **2114.0**	**-1043.7** **-2114.0**	**-7%** **-4%**	**1%** **-4%**

Once again, from Tab. 3, we can observe that the values obtained with the second order polynomial fit are closer to the experimental ones than the values using a linear fit. The errors that remain can be explained by the difficulty to measure small sag values on bare substrates and the possible small errors on deposited layer thickness.

CONCLUSIONS

We have validated a new thickness-dependent model for the stress induced in SiO_2 and Nb_2O_5 layers deposited by plasma assisted reactive magnetron sputtering (PARMS). This model was used to predict the evolution of the deformation of an optical component under manufacturing (e.g. a dielectric quarterwave mirror). From this accurate modeling, and the initial substrate deformation, it is thus possible to design a thin film stack that minimizes the deformation of the final component.

REFERENCES

[1] O. Adriani, S. Albergo, D. Alesini, M. Anania, D. Angal-Kalinin, et al.. Technical Design Report EuroGammaS proposal for the ELI-NP Gamma beam System. LAL/RT 14-63. 2014.
[2] C. A. Ur, “Gamma Beam System at ELI–NP”, AIP Conference Proceedings 1645, 237 (2015).
[3] M.-M. de Denus-Baillargeon, T. Schmitt, S. Larouche, and L. Martinu, "Design and fabrication of stress-compensated optical coatings: Fabry–Perot filters for astronomical applications," Appl. Opt. 53, 2616-2624 (2014)
[4] M. Scherer, J. Pistner, W. Lehnert, “UV- and VIS Filter Coatings by Plasma Assisted Reactive Magnetron Sputtering (PARMS)”, OIC 2010 Proceedings.
[5] T. Begou, F. Lemarchand and J. Lumeau, "Advanced optical interference filters based on metal and dielectric layers", accepted for publication in Optics Express (2016).
[6] A. Zoeller, M., H. Hagedorn, W. Klug and C. Schmitt, “High accurate in-situ optical thickness monitoring”, *OIC 2004 Proceedings*.
[7] G. Stoney, The tension of metallic films deposited by electrolysis, Proc. R. Soc. London, Ser. A 82, 172 (1909).
[8] T. Begou, H. Krol, D. Stojcevski, F. Lemarchand, M. Lequime, C. Grezes-Besset, J. Lumeau, “Complex optical interference filter with stress compensation”, SPIE 9627, Optical Systems Design 2015: Advances in Optical Thin Films V, 96270R (23 September 2015).
[9] F. Lemarquis, “Athermal compensation of the stress-induced surface deflection of optical coatings using iso-admittance layers”, Appl. Opt., vol.53 (4), pp. 229-236, February 2014.